



Paradoxical probabilistic behavior for strongly correlated many-body classical systems



Max Jauregui ^{a,*}, Constantino Tsallis ^{a,b}

^a Centro Brasileiro de Pesquisas Físicas and National Institute of Science and Technology for Complex Systems, Rua Xavier Sigaud 150, Rio de Janeiro 22290-180, RJ, Brazil

^b Santa Fe Institute, 1399 Hyde Park Road, Santa Fe, NM 87501, USA

ARTICLE INFO

Article history:

Received 12 February 2015

Accepted 17 April 2015

Available online 22 April 2015

Communicated by C.R. Doering

Keywords:

Strongly correlated system

q -Gaussian distribution

ABSTRACT

Using a simple probabilistic model, we illustrate that a small part of a strongly correlated many-body classical system can show a paradoxical behavior, namely asymptotic stochastic independence. We consider a triangular array such that each row is a list of n strongly correlated random variables. The correlations are preserved even when $n \rightarrow \infty$, since the standard central limit theorem does not hold for this array. We show that, if we choose a fixed number $m < n$ of random variables of the n th row and trace over the other $n - m$ variables, and then consider $n \rightarrow \infty$, the m chosen ones can, paradoxically, turn out to be independent. However, the scenario can be different if m increases with n . Finally, we suggest a possible experimental verification of our results near criticality of a second-order phase transition.

© 2015 Elsevier B.V. All rights reserved.

1. Introduction

As well known, sensible differences exist between quantum and classical correlations. The basic reason for that is that the quantum description of a many-body system allows the appearance of entangled states which do not have a clear classical counterpart. For instance, a study of a finite-length part of an infinitely long quantum spin chain has shown, among other things, that quantum correlations remain present in the subchain [1]. The correlations are strong enough to mandate the replacement of the additive von Neumann entropy for thermodynamical purposes. Indeed, that entropy is known to be nonextensive for such systems, whereas the nonadditive q -entropy [2] for a special value of the index q re-establishes the desirable thermodynamical extensivity. For a quantum critical phenomenon of a one-dimensional many-body model belonging to the universality class associated with the central charge c , the value of that index is given by

$$q = \frac{\sqrt{9 + c^2} - 3}{c}. \quad (1)$$

For instance, for the first-neighbor Ising ferromagnet in the presence of a transverse magnetic field, we have $c = 1/2$, hence $q = \sqrt{37} - 6 \simeq 0.08$.

The q -entropy associated with a density matrix ρ is defined by

* Corresponding author.

E-mail addresses: jauregui@cbpf.br (M. Jauregui), tsallis@cbpf.br (C. Tsallis).

$$S_q(\rho) := k \frac{1 - \text{tr} \rho^q}{q - 1}, \quad (2)$$

for any real $q \neq 1$ ($S_1(\rho) = -k \text{tr}(\rho \ln \rho)$ is the von Neumann entropy). This entropy is at the core of the so-called nonextensive statistical mechanics [2–4], which focuses on complex systems such as those involving long-range interactions or other sources of strong correlations (typically causing an ergodicity breakdown). Extremization of the q -entropy with appropriate constraints leads to the so-called q -exponential and q -Gaussian distributions. The q -exponential function is defined by

$$e_q^x := \begin{cases} [1 - (1 - q)x]^{1/(1-q)} & \text{for any real } q \neq 1 \\ e^x & \text{for } q = 1 \end{cases} \quad (3)$$

for any x such that $1 + (1 - q)x > 0$. The q -Gaussian distribution with real parameters $q < 3$ and $\beta > 0$ is characterized by the density

$$G_q(\beta, x) := \begin{cases} \frac{\sqrt{\beta}}{N_q} e_q^{-\beta x^2} & \text{if } 1 + (q - 1)\beta x^2 > 0 \\ 0 & \text{otherwise,} \end{cases} \quad (4)$$

where

$$N_q := \begin{cases} \frac{2^{\frac{3-q}{1-q}} [\Gamma(\frac{2-q}{1-q})]^2}{\sqrt{1-q} \Gamma(\frac{2(2-q)}{1-q})} & \text{for } q < 1 \\ \sqrt{\pi} & \text{for } q = 1 \\ \frac{\sqrt{\pi} \Gamma(\frac{3-q}{2(q-1)})}{\sqrt{q-1} \Gamma(\frac{1}{q-1})} & \text{if } 1 < q < 3. \end{cases} \quad (5)$$

From (4), we notice immediately that a q -Gaussian distribution has compact support whenever $q < 1$. If $1 \leq q < 3$, the support of a q -Gaussian distribution is the whole real line. By the way, let us mention that, if $\beta < 0$, q -Gaussian distributions are normalizable for $q \geq 3$.

Both the q -exponential and q -Gaussian distributions appear in a large number of natural, artificial and social systems, e.g., in long-range-interacting many-body classical Hamiltonian systems [5–7], cold atoms in dissipative optical lattices [8,9], dusty plasmas [10], in the study of the over-damped motion of interacting particles [11–13], in high energy physics [14–16] and in biology [17].

A subsystem of a correlated system is in principle expected to also be correlated, even in classical systems. For instance, let us consider the following triangular array of random variables which take the values 0 or 1:

$$\begin{matrix} X_{1,1} \\ X_{2,1} & X_{2,2} \\ \vdots & \vdots & \ddots \\ X_{n,1} & X_{n,2} & \cdots & X_{n,n} \\ \vdots & \vdots & \vdots & \ddots \end{matrix} \quad (6)$$

Each row can be thought as an outcome of the experiment of tossing n coins, where $X_{n,i} = 1$ if the i th coin falls head and $X_{n,i} = 0$ otherwise. For the distribution of the n th row of (6) we will use one introduced by Rodriguez et al. [18]. More precisely, fixed any list (x_1, \dots, x_n) formed with the digits 0 and 1 such that $x_1 + \dots + x_n = k$, we define

$$\mathbb{P}(X_{n,1} = x_1, \dots, X_{n,n} = x_n) := \frac{1}{Z_{q,n}} \binom{n}{k}^{-1} e_q^{-t_{q,n,k}^2}, \quad (7)$$

where $q < 1$ is a real parameter,

$$t_{q,n,k} := \frac{1}{\sqrt{1-q}} \left[1 - 2 \left(\frac{k+1}{n+2} \right) \right] \quad (8)$$

and

$$Z_{q,n} := \sum_{k=0}^n e_q^{-t_{q,n,k}^2}. \quad (9)$$

After some algebra, it follows from (7) that

$$\mathbb{P}(X_{n,i} = 1) = \mathbb{P}(X_{n,i} = 0) = \frac{1}{2}. \quad (10)$$

This implies that the random variables in each row of (6) are not independent since the right-hand side of (7) is *not* equal to $1/2^n$. Moreover, putting $S_n := X_{n,1} + \dots + X_{n,n}$, it can be verified that

$$\frac{(n+2)\sqrt{1-q}}{2} \mathbb{P}(S_n = k) \sim G_q(1, t_{q,n,k}) \quad (11)$$

as $n \rightarrow \infty$ (see Fig. 1). It becomes now transparent why we have adopted, for our illustration, the distribution in (7).

If we analyze the marginal probabilities of the first two random variables of the n th row of (6), we will observe that, analogously to the case of two spins in a quantum spin chain [1], these two random variables are correlated (see Fig. 2), which is something we may intuitively expect. However, as we will see later on, this property does not necessarily follow from the fact that the random variables in each row of (6) are strongly correlated.

2. A paradoxical result

Suppose now that we have the array (6) and the distribution given in (7), but this time with $q \geq 1$ and

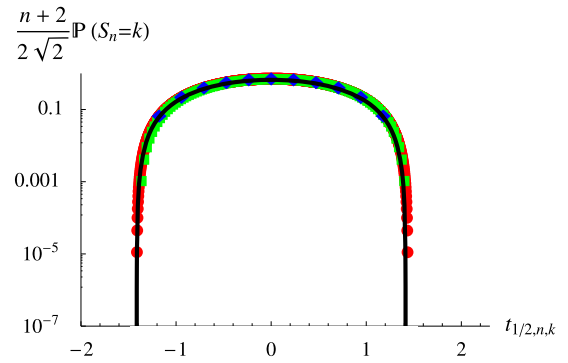


Fig. 1. Representation of $\frac{(n+2)}{2\sqrt{2}} \mathbb{P}(S_n = k)$ as a function of $t_{1/2,n,k}$ for $n = 10, 100$ and 1000 , where we have considered $q = 1/2$. The solid curve represent the right-hand side of (11).

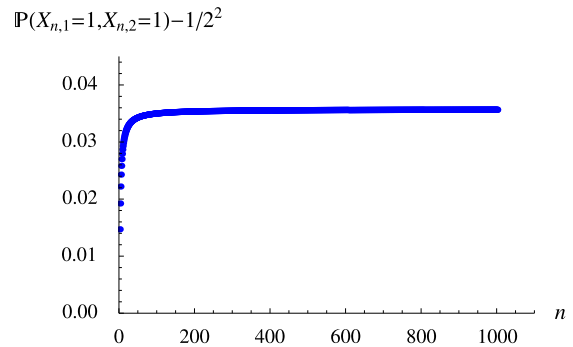


Fig. 2. Representation of $\mathbb{P}(X_{n,1} = 1, X_{n,2} = 1) - 1/2^2$ as a function of n for $q = 1/2$. We see that the curve goes away from 0 as n increases. This numerical result is confirmed by the $q = 0$ case, which turns out to be analytically tractable, and provides $\mathbb{P}(X_{n,1} = 1, X_{n,2} = 1) - 1/2^2 = 1/20, \forall n$. The present available results are consistent with a value of $\lim_{n \rightarrow \infty} [\mathbb{P}(X_{n,1} = 1, X_{n,2} = 1) - 1/2^2]$ which approaches zero for q approaching one from below.

$$t_{q,n,k} := \sqrt{n+1} \left(\frac{k+1}{n+2} - \frac{1}{2} \right). \quad (12)$$

It follows immediately from (7) that, as in the $q < 1$ case,

$$\begin{aligned} \mathbb{P}(X_{n,\pi(1)} = x_1, \dots, X_{n,\pi(n)} = x_n) \\ = \mathbb{P}(X_{n,1} = x_1, \dots, X_{n,n} = x_n) \end{aligned} \quad (13)$$

for any permutation π of $\{1, \dots, n\}$. This allows us to use the reduced notation

$$r_{q,n,k} := \mathbb{P}(X_{n,1} = x_1, \dots, X_{n,n} = x_n), \quad (14)$$

where (x_1, \dots, x_n) is any list formed with the digits 0 and 1 such that $x_1 + \dots + x_n = k$. Moreover, it follows from (13) that

$$s_{q,n,k} := \mathbb{P}(S_n = k) = \binom{n}{k} r_{q,n,k}. \quad (15)$$

Let us incidentally mention that, for $q > 1$, it has been shown [19,20] that the corresponding large deviation theory involves q -exponentials instead of the standard exponentials. More precisely, it has been shown numerically that, as n increases, the probability of large deviations $\mathbb{P}(S_n \leq nx)$, $x < 1/2$, decay to zero like a q' -exponential, where $q' > 1$ is some function $q'(q)$ such that $q'(1) = 1$, thus recovering the usual theory.

Also, it follows from (12) that $t_{q,n,n-k} = -t_{q,n,k}$ and, consequently, $r_{q,n,n-k} = r_{q,n,k}$. This implies that $\mathbb{P}(S_n \leq nx) = \mathbb{P}(S_n \geq n(1-x))$ for every $x < 1/2$. The fact that these probabilities converge to zero as $n \rightarrow \infty$ means that the weak law of large numbers holds for (6). It is easy to see from (7) that $r_{q,n,k} \neq r_{q,n+1,k} +$

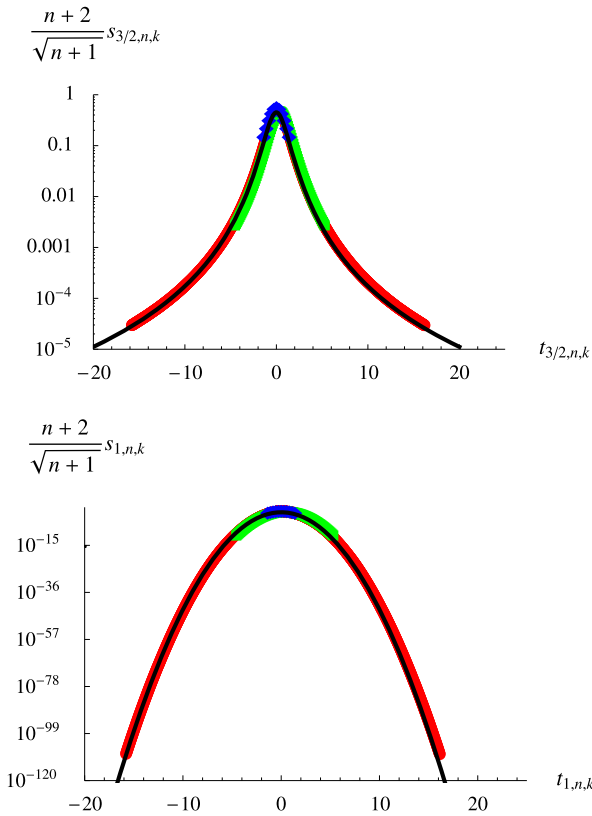


Fig. 3. Representation of $\frac{n+2}{\sqrt{n+1}} S_{q,n,k}$ as a function of $t_{q,n,k}$ for $n = 10, 100$ and 1000 , where we have considered $q = 3/2$ (top) and $q = 1$ (bottom). In both cases, the solid curves represent the right-hand side of (16).

$r_{q,n+1,k+1}$. Nevertheless, it has been verified [18] that the equality (Leibniz triangle rule) holds asymptotically when $n \rightarrow \infty$, i.e., $\lim_{n \rightarrow \infty} \frac{r_{q,n+1,k} + r_{q,n+1,k+1}}{r_{q,n,k}} = 1$.

Also for $q \geq 1$, (10) holds, meaning that the random variables in each row of (6) are not independent. Moreover, the distribution of S_n , after appropriate scaling, approximates, as n increases, to a q -Gaussian distribution with parameters $q \geq 1$ and $\beta = 1$ [19]. More precisely,

$$\frac{n+2}{\sqrt{n+1}} S_{q,n,k} \sim G_q(1, t_{q,n,k}) \tag{16}$$

for large values of n (see Fig. 3).

For $n > 1$, let us focus on the analysis of $m < n$ random variables of the n th row of (6). Given any list (x_1, \dots, x_m) formed with the numbers 0 and 1 such that $x_1 + \dots + x_m = l$, we obtain from (7) that the marginal probabilities are given by

$$\begin{aligned} \mathbb{P}(X_{n,1} = x_1, \dots, X_{n,m} = x_m) \\ = \frac{1}{Z_{q,n}} \sum_{j=0}^{n-m} \binom{n-m}{j} \binom{n}{j+l}^{-1} e_q^{-t_{q,n,j+l}^2}. \end{aligned} \tag{17}$$

By virtue of (13), the joint distribution of any subset containing m random variables of the n th row of (6) is given by the right-hand side of (17). In order to simplify the notation, we will use

$$p_{q,n,m} := \mathbb{P}(X_{n,1} = 1, \dots, X_{n,m} = 1). \tag{18}$$

We numerically verify that $p_{q,n,2}$ approaches $1/2^2$ as n increases (see Fig. 4). This implies that any two variables of rows of (6) that are sufficiently far below are, surprisingly enough, asymptotically independent. This appears to be, in the present

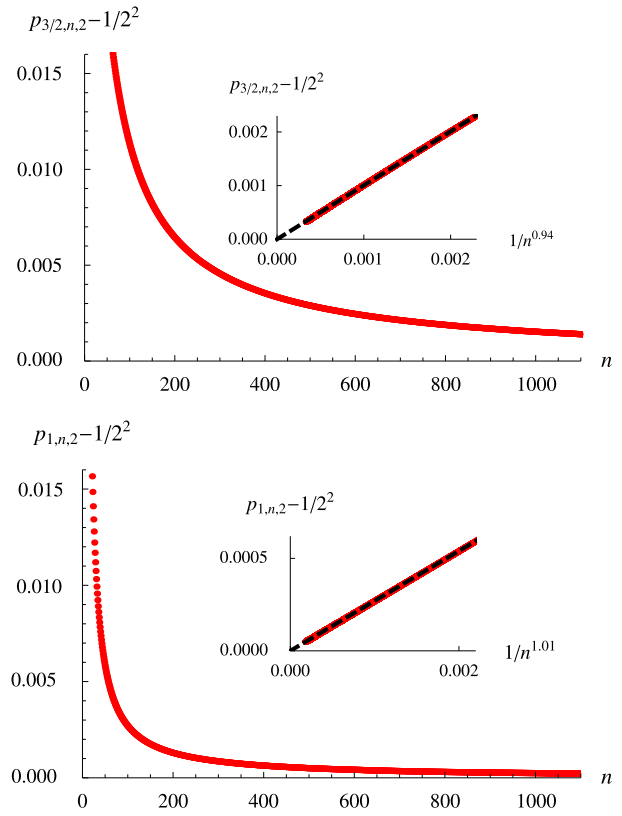


Fig. 4. Representation of $p_{q,n,2} - 1/2^2$ as a function of n , where we have considered $q = 3/2$ (top) and $q = 1$ (bottom). In both cases we notice that $p_{q,n,2}$ approaches $1/2^2$ as n increases. The insets suggest that $p_{q,n,2} - 1/2^2$ decay to zero like a power law in both cases. The exponent of n appears to slightly depend on q : see also Fig. 5.

case, the reason why the law of large numbers holds for (6). Indeed, pairwise independence is sufficient for this law to emerge [21]. Moreover, fixing $m > 0$, it can be verified that

$$\begin{aligned} \text{Var}(X_{n,1} + \dots + X_{n,m}) \\ = m \left(\frac{1}{2} - p_{q,n,2} \right) + m^2 \left(p_{q,n,2} - \frac{1}{4} \right), \end{aligned} \tag{19}$$

which, as n increases, approaches the value corresponding to independence, namely $m/2$.

If instead of choosing a pair of random variables, we choose $m > 2$ ones from the n th row of (6), we will obtain that $p_{q,n,m}$ approaches $1/2^m$ as n increases, as illustrated in Fig. 5. This implies, like in the case $m = 2$, that the correlations among m random variables of a row of (6) asymptotically vanish if $n \rightarrow \infty$. However, the scenario seems to be different if we choose m_n random variables of the n th row of (6), where m_1, m_2, \dots is some increasing sequence of positive integers with $m_n \leq n$ (see Figs. 6 and 7). This is something that is not surprising since the n th row of (6) does not become independent as $n \rightarrow \infty$; otherwise (6) would obey the standard central limit theorem, contradicting (16).

3. Final remarks and conclusions

We conclude that, for $q \geq 1$ (i.e., unbounded support), if we are restricted to analyze a prefixed finite number of random variables in each row of (6), it is, for the present model, impossible to decide whether the chosen random variables are part of an independent or a correlated superset of random variables. However, this ambiguity is removed if we focus on a number of random variables which increases with n .

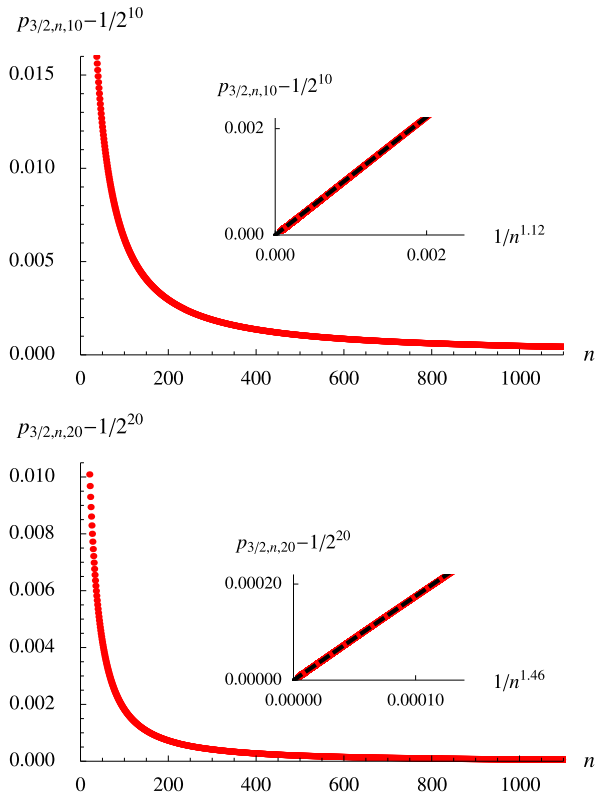


Fig. 5. Representation of $p_{3/2,n,9} - 1/2^9$ (top) and $p_{3/2,n,20} - 1/2^{20}$ (bottom) as functions of n . The insets suggest that both functions decay to zero like a power law. The exponent of n appears to depend on m for a given value of q .

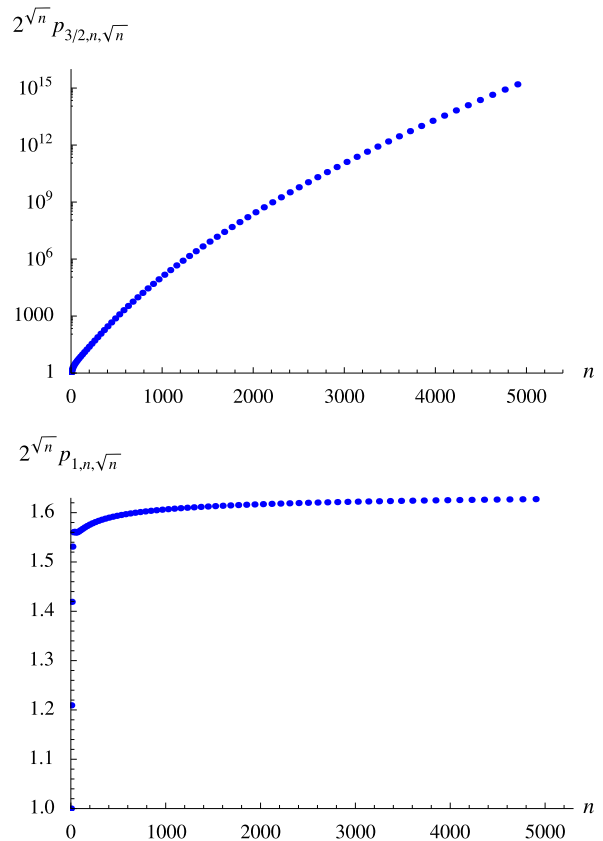


Fig. 7. Representation of the ratio of $p_{q,n,\sqrt{n}}$ and $1/2^{\sqrt{n}}$ as a function of n for $q = 3/2$ (top) and $q = 1$ (bottom). Clearly, this ratio is different from 1 when n is very large. To construct this graph, we have considered perfect squares for n .

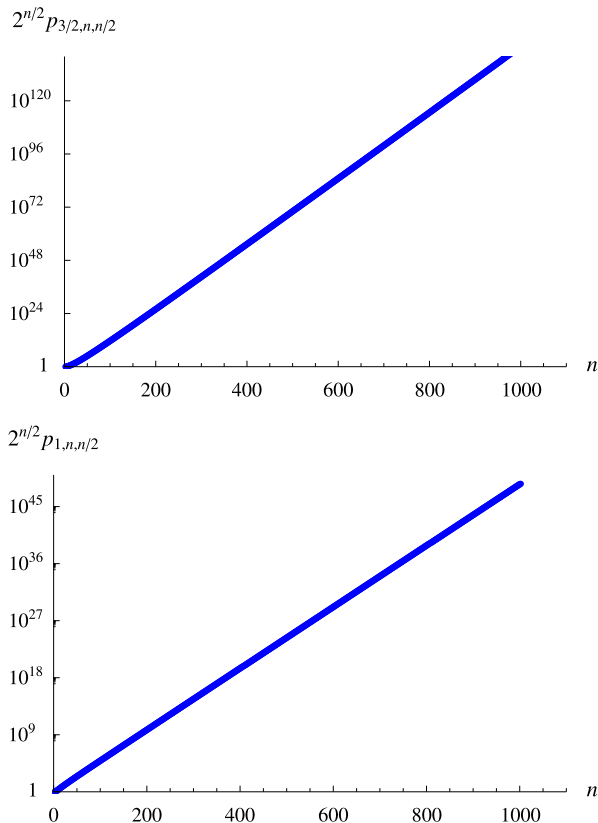


Fig. 6. Representation of the ratio of $p_{q,n,n/2}$ and $1/2^{n/2}$ as a function of n for $q = 3/2$ (top) and $q = 1$ (bottom). Clearly, this ratio is increasingly different from 1 when n is very large. To construct this graph, we have considered even values of n .

In science, in many circumstances, we want to analyze a growing system; for instance, the evolution of a microbiological culture, the propagation of an epidemic, among others. However, sometimes by technical difficulties, we are just allowed to study parts of the system with a determined size, which is much smaller than the size of the whole system. Naturally, we can think that analyzing several parts of that size can be sufficient to reach a conclusion about the whole system. However, as we have seen, this procedure may lead to the statement of false claims about the entire system, specially if strong correlations are present in it. In contrast, the results obtained by looking at a growing part of the system may be generalized to the whole system.

As a physical illustration of the present paradoxical results, we suggest the following experiment. Consider a macroscopic sample of some material which presents a second-order phase transition. We will perform measurements (e.g., magnetic or electric susceptibility) on a part with fixed size of the large sample. This part can be macroscopic as well but much smaller than the whole sample. As we adjust the temperature of the sample to values near the critical one, the correlation length increases and eventually surpasses the size of the part we are focusing on. At this stage, the microscopic constituents in the whole sample clearly are strongly correlated. However, this correlation might, interestingly enough, *not* be detectable in the subsystem that we are studying.

Let us finally emphasize that the present surprising effects possibly are linked to the classical nature of the system, and to the fact that the support of the attractor is unbounded. Indeed, quantum correlations, as well as classical ones with bounded support, are of a different nature, and therefore these correlations do persist at the level of a part of the system, even if the size of the entire system keeps increasing.

Acknowledgements

We acknowledge L.J.L. Cirto and E.M.F. Curado for fruitful discussions. Partial financial support from CNPq and FAPERJ (Brazilian agencies) are also acknowledged. One of us (C.T.) has also benefited from partial financial support from the John Templeton Foundation.

References

- [1] F. Caruso, C. Tsallis, Nonadditive entropy reconciles the area law in quantum systems with classical thermodynamics, *Phys. Rev. E* 78 (2008) 021102.
- [2] C. Tsallis, Possible generalization of the Boltzmann–Gibbs statistics, *J. Stat. Phys.* 52 (1988) 479–487.
- [3] M. Gell-Mann, C. Tsallis, *Nonextensive Entropy – Interdisciplinary Applications*, Oxford University Press, New York, 2004.
- [4] C. Tsallis, *Introduction to Nonextensive Statistical Mechanics: Approaching a Complex World*, Springer, New York, 2009.
- [5] A. Pluchino, A. Rapisarda, C. Tsallis, Nonergodicity and central-limit behavior for long-range Hamiltonians, *Europhys. Lett.* 80 (2007) 26002.
- [6] L.J.L. Cirto, V.R.V. Assis, C. Tsallis, Influence of the interaction range on the thermostatics of a classical many-body system, *Physica A* 393 (2015) 286.
- [7] H. Christodoulidi, C. Tsallis, T. Bountis, Fermi–Pasta–Ulam model with long-range interactions: dynamics and thermostatics, *Europhys. Lett.* 108 (2014) 40006.
- [8] P. Douglas, S. Bergamini, F. Renzoni, Tunable Tsallis distributions in dissipative optical lattices, *Phys. Rev. Lett.* 96 (2006) 110601.
- [9] E. Lutz, F. Renzoni, Beyond Boltzmann–Gibbs statistical mechanics in optical lattices, *Nat. Phys.* 9 (2013) 615.
- [10] B. Liu, J. Goree, Superdiffusion and non-Gaussian statistics in a driven-dissipative 2D dusty plasma, *Phys. Rev. Lett.* 100 (2008) 055003.
- [11] J.S. Andrade Jr., G.F.T. da Silva, A.A. Moreira, F.D. Nobre, E.M.F. Curado, Thermostatistics of overdamped motion of interacting particles, *Phys. Rev. Lett.* 105 (2010) 260601.
- [12] M.S. Ribeiro, F.D. Nobre, E.M.F. Curado, Overdamped motion of interacting particles in general confining potentials: time-dependent and stationary-state analyses, *Eur. Phys. J. B* 85 (2012) 399.
- [13] M.S. Ribeiro, F.D. Nobre, E.M.F. Curado, Time evolution of interacting vortices under overdamped motion, *Phys. Rev. E* 85 (2012) 021146.
- [14] C.Y. Wong, G. Wilk, Tsallis fits to p_t spectra for pp collisions at the LHC, *Acta Phys. Pol. B* 43 (2012) 2047.
- [15] C.Y. Wong, G. Wilk, Tsallis fits to p_t spectra and multiple hard scattering in pp collisions at the LHC, *Phys. Rev. D* 87 (2013) 114007.
- [16] L.J.L. Cirto, C. Tsallis, C.Y. Wong, G. Wilk, The transverse-momenta distributions in high-energy pp collisions – a statistical-mechanical approach, arXiv: 1409.3278, 2014.
- [17] A. Upadhyaya, J.P. Rieu, J.A. Glazier, Y. Sawada, Anomalous diffusion and non-Gaussian velocity distribution of Hydra cells in cellular aggregates, *Physica A* 293 (2001) 549.
- [18] A. Rodríguez, V. Schwämmle, C. Tsallis, Strictly and asymptotically scale invariant probabilistic models of n correlated binary random variables having q -Gaussians as $n \rightarrow \infty$ limiting distributions, *J. Stat. Mech.* (2008) P09006.
- [19] G. Ruiz, C. Tsallis, Towards a large deviation theory for strongly correlated systems, *Phys. Lett. A* 376 (2012) 2451.
- [20] G. Ruiz, C. Tsallis, Reply to comment on “Towards a large deviation theory for strongly correlated systems”, *Phys. Lett. A* 377 (2013) 491.
- [21] R. Durrett, *Probability: Theory and Examples*, 4th edition, Cambridge University Press, New York, 2010.